

## Electronic Supplementary Information

# Few-Layered CuInP<sub>2</sub>S<sub>6</sub> Nanosheet with Sulfur Vacancy Boosting Photocatalytic Hydrogen Evolution

Peng Yu,<sup>a,b</sup> Fengmei Wang,<sup>\*b</sup> Jun Meng,<sup>c</sup> Tofik Ahmed Shifa,<sup>b</sup> Marshet Getaye

Sendeku,<sup>b</sup> Ju Fang,<sup>d</sup> Shuxian Li,<sup>d</sup> Zhongzhou Cheng,<sup>b</sup> Xiaoding Lou<sup>\*a</sup> and Jun He<sup>b</sup>

<sup>a</sup> Engineering Research Center of Nano-Geomaterials of Ministry of Education, Faculty of Materials Science and Chemistry, China University of Geosciences, Wuhan 430074, China. E-mail: [louxiaoding@cug.edu.cn](mailto:louxiaoding@cug.edu.cn)

<sup>b</sup> CAS Center for Excellence in Nanoscience, CAS Key Laboratory of Nanosystem and Hierarchical Fabrication, National Center for Nanoscience and Technology, Beijing 100190, China. E-mail: [wangfm@nanoctr.cn](mailto:wangfm@nanoctr.cn)

<sup>c</sup> Division of Interfacial Water and Key Laboratory of Interfacial Physics and Technology, Shanghai Institute of Applied Physics, Chinese Academy of Sciences, Shanghai 201800, China

<sup>d</sup> School of Physics and Technology, Key Laboratory of Artificial Micro- and Nano-structures of Ministry of Education, Wuhan University, Wuhan, 430072, China

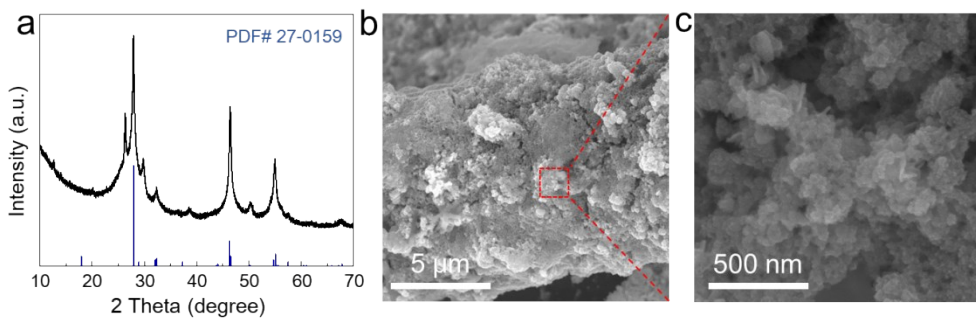


**Fig. S1** (a) XRD pattern of  $\text{CuInS}_x/\text{CFs}$  precursor. (b, c) SEM images of  $\text{CuInS}_x$  nanocrystal on the carbon fibers and corresponding partial enlarged image.

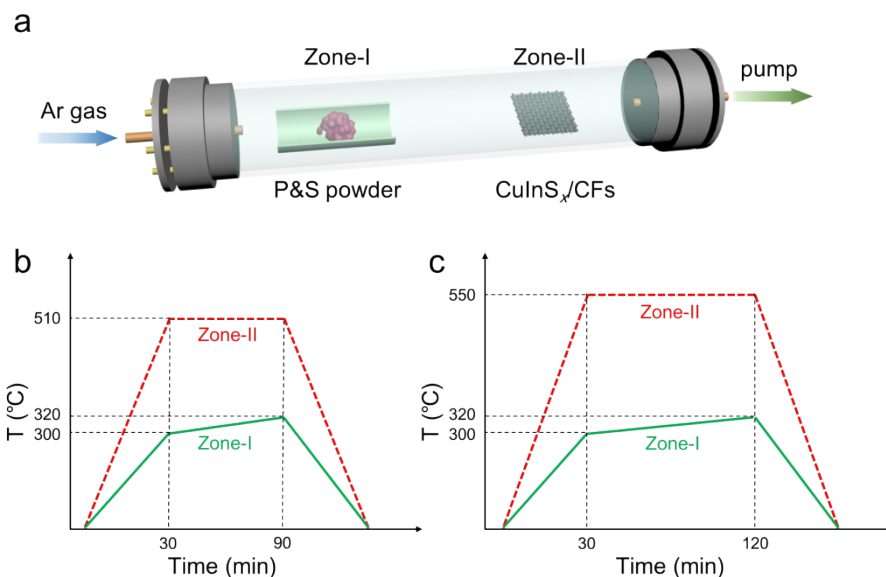


**Fig. S2** (a) Schematic diagram of chemical vapor conversion synthesis of CIPS crystals on the carbon fibers. (b, c) The heating procedure profile for growing CIPS NSs (b) and CIPS MSs (c). In details, first, the P&S powder (Zone- I ) is heated to 300 °C within 30 min, while the  $\text{CuInS}_x/\text{CFs}$  (Zone- II ) is heated to 510 and 550 °C for synthesizing CIPS NSs and MSs, respectively. And then, the zone- I is heated to 320 °C finally within 60 min for CIPS NSs and 90 min for CIPS MSs synthesis at 510 and 550 °C, respectively. Finally, after the heating procedure is completed, it is naturally cooled to room temperature.

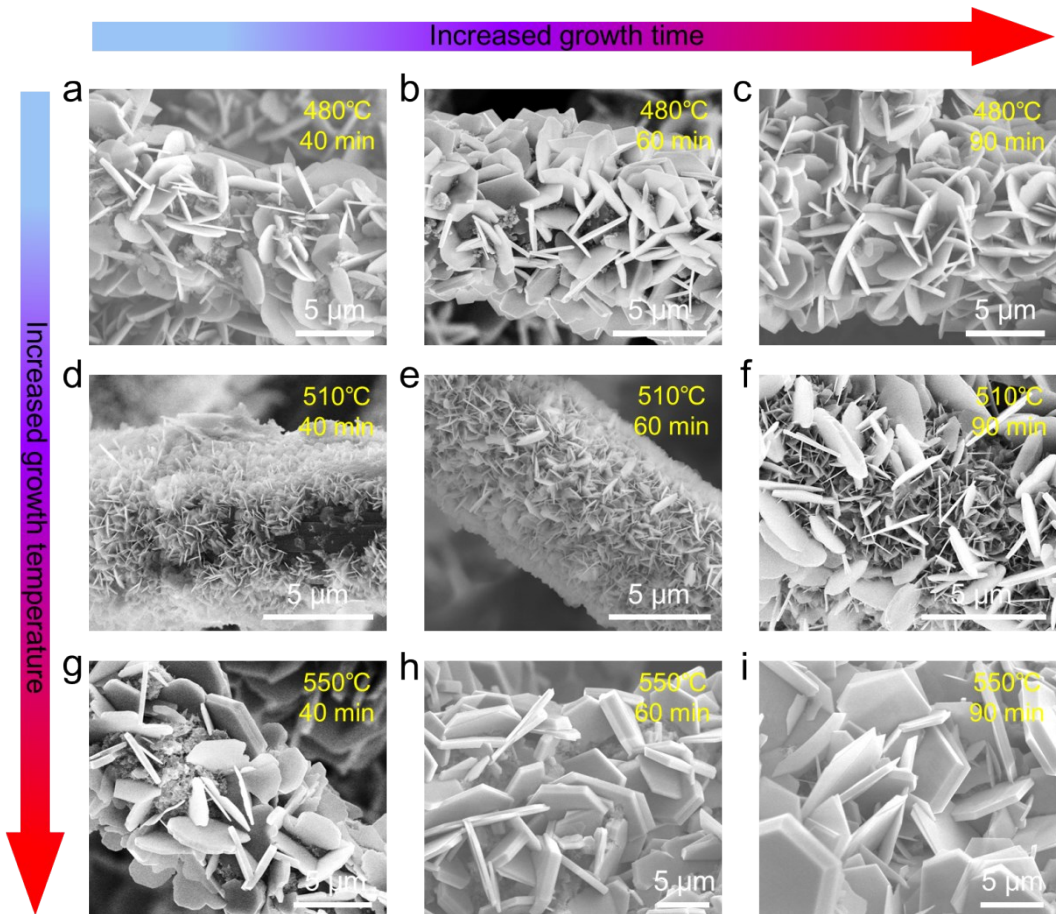


**Fig. S3** SEM images of different synthesized CIPS sheets under various growth parameters. The CIPS sheets synthesized at 480 °C (a-c), 510 °C (d-f) and 550 °C (g-i) within different reaction times of 40 min, 60 min and 90 min, respectively. If the growth time is shorter than 40 min, we found that a mixture of residual precursors and unevenly distributed CIPS sheets on the carbon fibers at 480 °C. But, if the synthesis was conducted at high reaction temperature (550 °C) within longest time (90 min), some thick CIPS sheets would be obtained. Thus, the carefully control of the reaction time and temperature is critical for synthesizing CIPS nanosheets. Applying suitable reaction time, like 60 min, and temperature (510 °C), the uniform CIPS nanosheets can be synthesized and covered the carbon fibers.

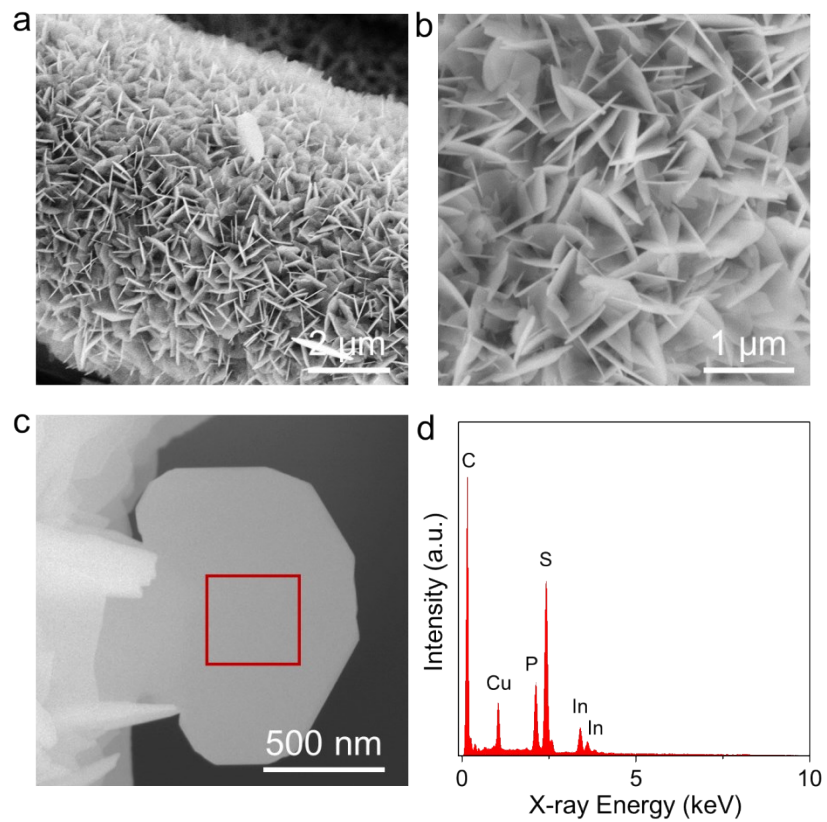


**Fig. S4** (a-c) SEM images of CIPS NSs synthesized at 510 °C within 60 min. (d) Corresponding EDX spectrum collected from marked region in c.

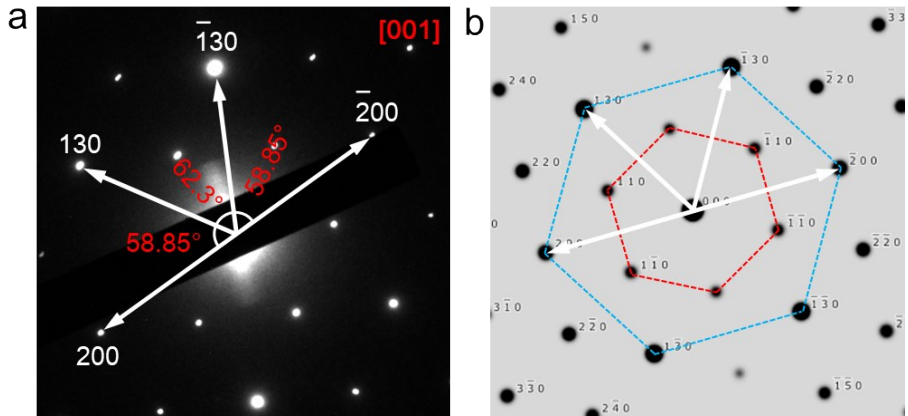


**Fig. S5** (a) SAED pattern of CIPS NSs (b) Simulated pattern based on the standard Cif file of monoclinic CIPS crystal by using the CrystalDiffract software.

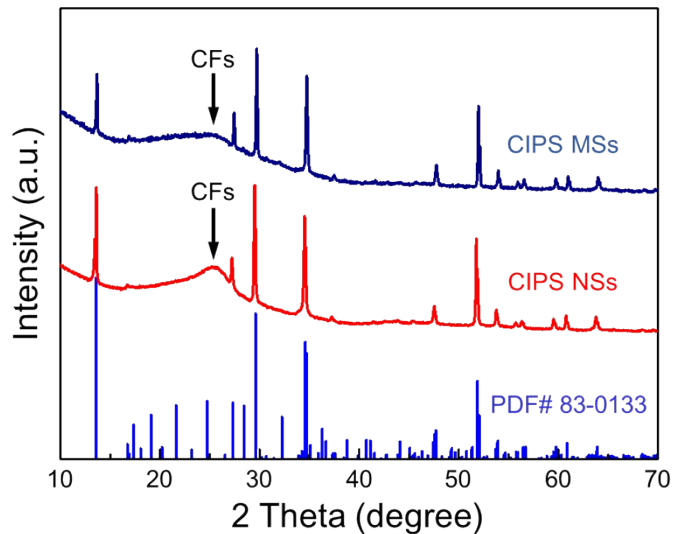


**Fig. S6** XRD patterns of the CIPS MSs and NSs on the carbon fibers.

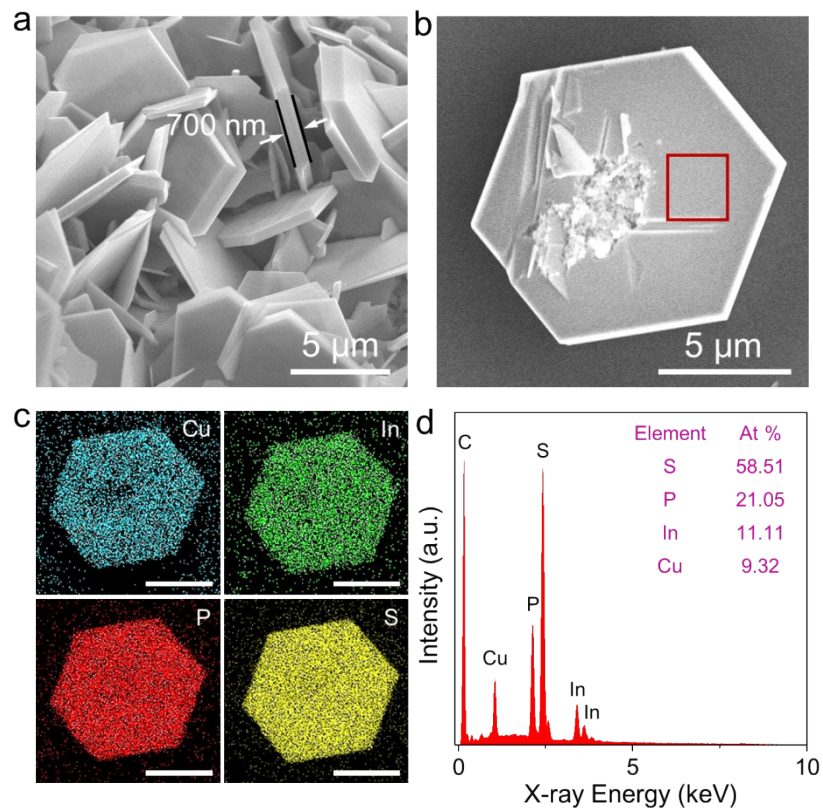


**Fig. S7** (a, b) SEM images of the as-prepared CIPS MSs on the carbon fibers (a) and single CIPS microsheet (b). (c) EDX elemental mapping of CIPS MSs and (d) EDX spectrum of CIPS MSs with the atomic ratio of Cu: In: P: S nearly to 1: 1: 2: 6 collected from marked region in b.

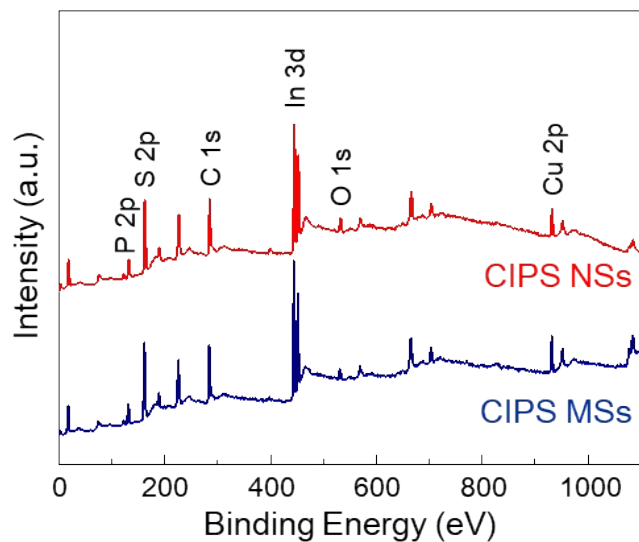


**Fig. S8** Comparison of XPS spectra of the CIPS MSs and NSs.

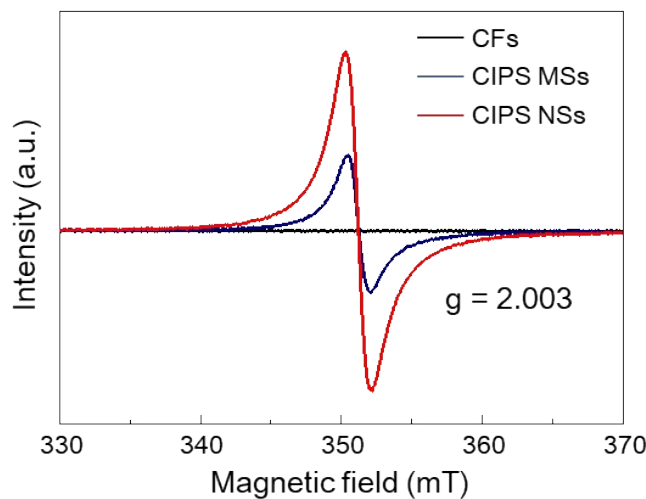


**Fig. S9** Room-temperature ESR spectra of the CIPS MSs and NSs, in which the signal at  $g = 2.003$  corresponds to the sulfur vacancies.

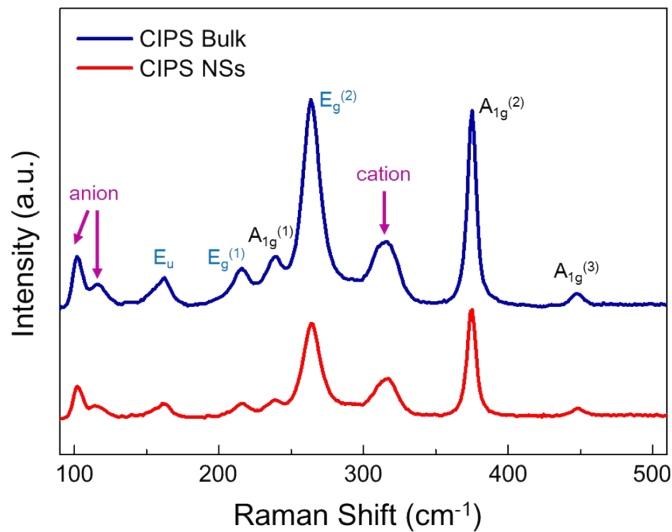


**Fig. S10** Raman spectra of the CIPS MSs and NSs at room temperature, where the cation and anion are  $\text{Cu}^+$ ,  $\text{In}^{3+}$  and  $[\text{P}_2\text{S}_6]^{4-}$ , respectively.

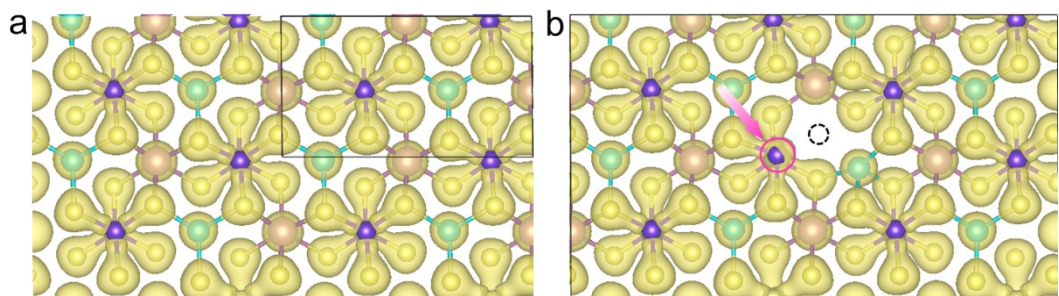


**Fig. S11** Charge density distributions of CIPS monolayer (a) and S defective CIPS monolayer (b). Isosurface level equals to 0.1.

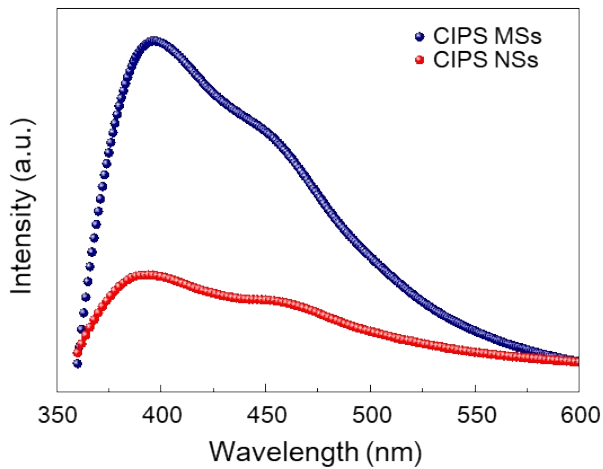


**Fig. S12** Room-temperature PL spectra of the CIPS MSs and NSs using the excitation laser with the wavelength of 320 nm.

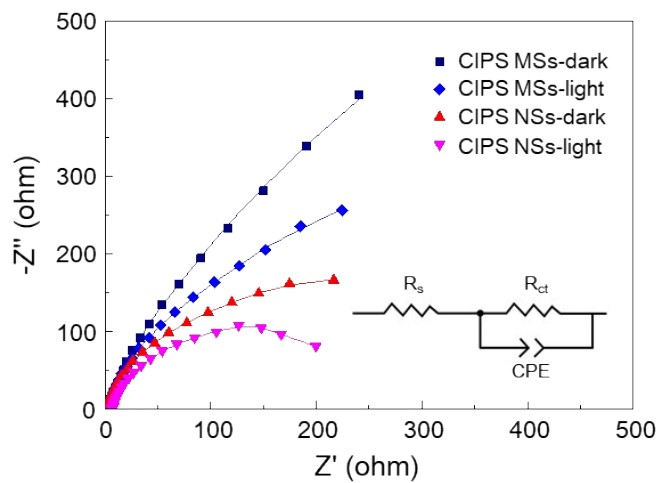


**Fig. S13** Electrochemical impedance spectra collected on the CIPS MS and NS electrodes in the 0.5 M  $\text{Na}_2\text{SO}_4$  aqueous solution without light (dark) and with Xe light illumination ( $\lambda > 300$  nm,  $200 \text{ mW cm}^{-2}$ ).

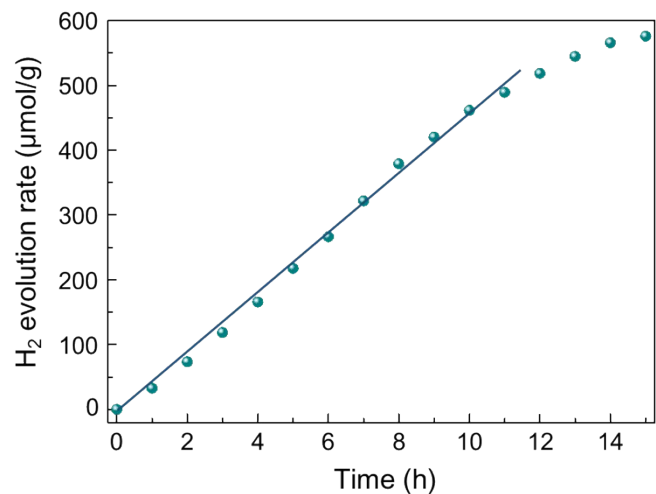


**Fig. S14** Photocatalytic  $H_2$  evolution of CIPS NSs from pure water under Xe light illumination ( $\lambda > 300$  nm,  $400 \text{ mW cm}^{-2}$ ).

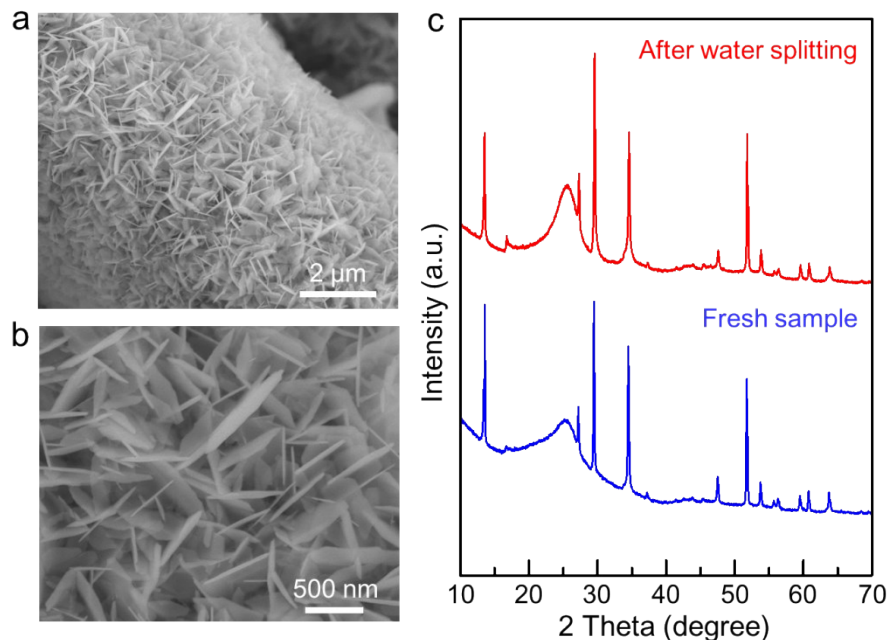


**Fig. S15** (a-b) SEM images of CIPS NSs on carbon fibers after continuously 15 h hydrogen evolution in pure water under Xe light illumination.

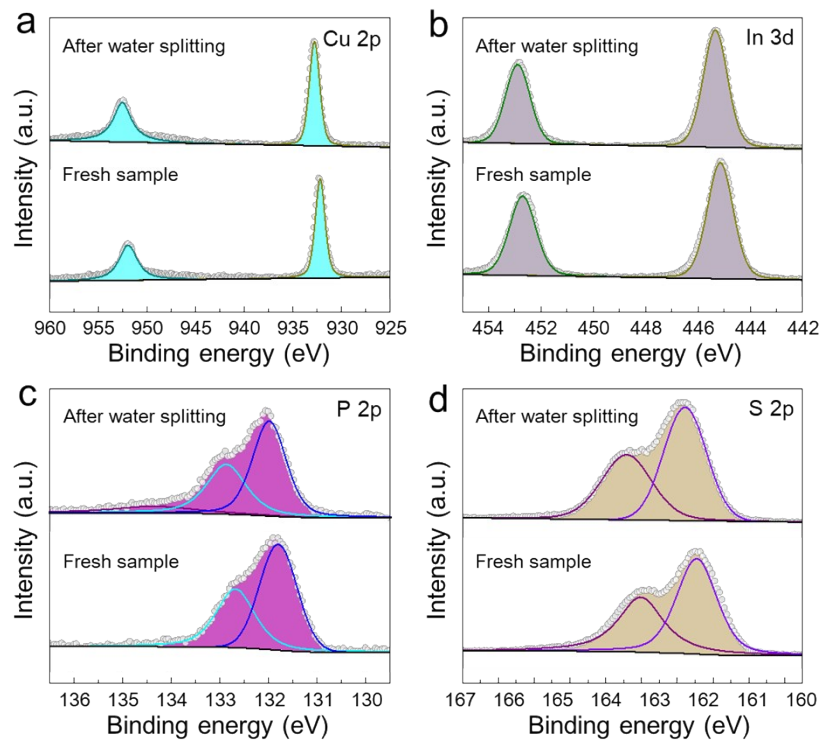


**Fig. S16** XPS spectra of CIPS NSs compared with the fresh sample in Cu 2p (a), In 3d (b), P 2p (c) and S 2p (d) regions after conducting photocatalytic water splitting in pure water under Xe light illumination.

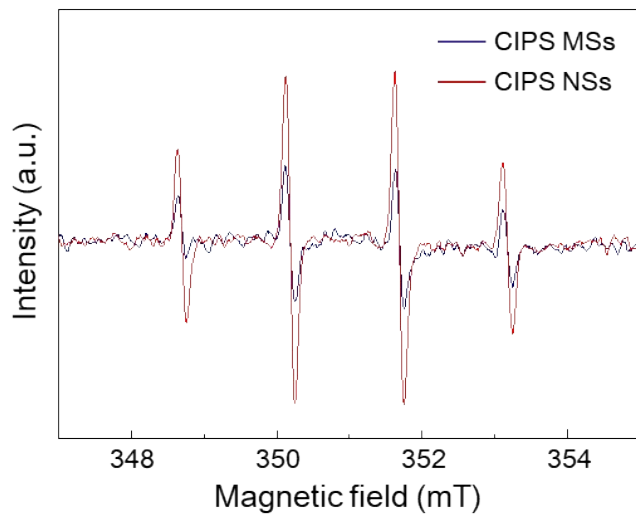


**Fig. S17** ESR responses of the DMPO-OH spin adduct in the CIPS MSs and NSs photocatalyst.

**Table S1** Lifetime parameters of time-resolved photoluminescence of CIPS MSs and NSs under 320 nm excitation.

Samples	$\tau_1$ (ns)	$A_1$ (%)	$\tau_2$ (ns)	$A_2$ (%)	$\tau_A$ (ns)
CIPS MSs	0.236	93.85	4.056	6.15	2.26
CIPS NSs	0.320	85.81	4.508	14.19	3.25

**Table S2** Comparison of the photocatalytic H<sub>2</sub> evolution performance of various MPX<sub>3</sub>.

Photocatalyst	Morphology	Light source	Reaction conditions	H <sub>2</sub> evolution rate (μmol g <sup>-1</sup> h <sup>-1</sup> )	Ref.
CuInP <sub>2</sub> S <sub>6</sub>	nanosheets	300 W Xe lamp	0.1 M Na <sub>2</sub> S&Na <sub>2</sub> SO <sub>3</sub> aqueous solution	804 46	This work
	microsheets		pure water		
NiPS <sub>3</sub>	nanosheets	300 W Xe lamp	0.1 M Na <sub>2</sub> S&Na <sub>2</sub> SO <sub>3</sub> aqueous solution	100 74.67	1
			pure water		
MnPS <sub>3</sub>	nanosheets	AM 1.5 solar light	0.35 M Na <sub>2</sub> S&0.25 M Na <sub>2</sub> SO <sub>3</sub> aqueous solution	26.42 6.46	1
			pure water		
MnPSe <sub>3</sub>	nanosheets	AM 1.5 solar light	0.35 M Na <sub>2</sub> S&0.25 M Na <sub>2</sub> SO <sub>3</sub> aqueous solution	21.2 43.5	2
			pure water		
FePSe <sub>3</sub>	quantum sheets	300 W Xe lamp	10 vol % TEOA aqueous solution	94 36.1	3
			pure water		
			10 vol % TEOA aqueous solution	290	
			pure water	89.7	

**Table S3.** Comparison of the photocatalytic H<sub>2</sub> evolution performance with other 2D layered materials.

Photocatalyst	Morphology	Light source	Reaction conditions	H <sub>2</sub> evolution rate (μmol g <sup>-1</sup> h <sup>-1</sup> )	Ref.
CuInP <sub>2</sub> S <sub>6</sub>	nanosheets	300 W Xe lamp	0.1 M Na <sub>2</sub> S&Na <sub>2</sub> SO <sub>3</sub> aqueous solution	804	This work
	microsheets	300 W Xe lamp	0.1 M Na <sub>2</sub> S&Na <sub>2</sub> SO <sub>3</sub> aqueous solution	100	
Graphitic carbon nitride (g-C <sub>3</sub> N <sub>4</sub> )	carbon nanodot-carbon nitride	300 W Xe lamp with 420 nm cut-off filter	Pure Water	105	4
	half-metallic carbon nitride nanosheets	AM 1.5 solar light	10 vol % TEOA aqueous solution	1009	5
	porous P-doped graphitic carbon nitride nanosheets	300 W Xe lamp with 400 nm cut-off filter	20 vol % TEOA aqueous solution, 1 wt% Pt cocatalysts	1596	6
Black phosphorus (BP)	few layered BP nanosheets	300 W Xe lamp with 420 nm cut-off filter	15 vol % TEOA acetonitrile solution	64	7
	BP nanosheets	300 W Xe lamp with 420 nm cut-off filter	0.75 M Na <sub>2</sub> S&1.05 M Na <sub>2</sub> SO <sub>3</sub> aqueous solution	512	8
	Co-P/BP nanosheets	300 W Xe lamp with 420 nm cut-off filter	pure water	375	9
	nanohybrid of 2D BP/g-CN nanosheets	300 W mercury vapor lamp with 420 nm cut-off filter	20 vol % methanol aqueous solution	427	10
Transition metal dichalcogenides (TMDs)	SnS <sub>2</sub> nanoplates	400 W Xe lamp with 420 nm cut-off filter	0.1 M Na <sub>2</sub> S&Na <sub>2</sub> SO <sub>3</sub> aqueous solution 1 wt% Pt cocatalysts	1306	11
	SnS <sub>2</sub> nanoplates	300 W Xe lamp with 420 nm cut-off filter	50 mM ascorbic acid aqueous solution	356	12
Metal oxyhalides (MOX)	Fe modified BiOCl nanosheets	300 W Xe lamp with 420 nm cut-off filter	0.1 M Na <sub>2</sub> SO <sub>4</sub> aqueous solution	141.6	13
	BiOI hierarchical microspheres	350 W Xe lamp with 400 nm cut-off filter	deionized water with pH 7	1316.9	14

## References

1. F. Wang, T. A. Shifa, P. He, Z. Cheng, J. Chu, Y. Liu, Z. Wang, F. Wang, Y. Wen, L. Liang and J. He, *Nano Energy*, 2017, **40**, 673-680.
2. T. A. Shifa, F. Wang, Z. Cheng, P. He, Y. Liu, C. Jiang, Z. Wang and J. He, *Adv. Funct. Mater.*, 2018, **28**, 1800548.
3. Z. Cheng, T. A. Shifa, F. Wang, Y. Gao, P. He, K. Zhang, C. Jiang, Q. Liu and J. He, *Adv. Mater.*, 2018, **30**, 1707433.
4. J. Liu, Y. Liu, N. Liu, Y. Han, X. Zhang, H. Huang, Y. Lifshitz, S. T. Lee, J. Zhong and Z. Kang, *Science*, 2015, **347**, 970-974.
5. G. Zhou, Y. Shan, Y. Hu, X. Xu, L. Long, J. Zhang, J. Dai, J. Guo, J. Shen, S. Li, L. Liu and X. Wu, *Nat. Commun.*, 2018, **9**, 3366.
6. J. Ran, T. Y. Ma, G. Gao, X. W. Du and S. Z. Qiao, *Energy Environ. Sci.*, 2015, **8**, 3708-3717.
7. S. K. Muduli, E. Varrla, Y. Xu, S. A. Kulkarni, A. Katre, S. Chakraborty, S. Chen, T. C. Sum, R. Xu and N. Mathews, *J. Mater. Chem. A*, 2017, **5**, 24874-24879.
8. X. Zhu, T. Zhang, Z. Sun, H. Chen, J. Guan, X. Chen, H. Ji, P. Du and S. Yang, *Adv. Mater.*, 2017, **29**, 1605776.
9. B. Tian, B. Tian, B. Smith, M. C. Scott, R. Hua, Q. Lei and Y. Tian, *Nat. Commun.*, 2018, **9**, 1397.
10. M. Zhu, S. Kim, L. Mao, M. Fujitsuka, J. Zhang, X. Wang and T. Majima, *J. Am. Chem. Soc.*, 2017, **139**, 13234-13242.
11. S. R. Damkale, S. S. Arbuj, G. G. Umarji, R. P. Panmand, S. K. Khore, R. S.

- Sonawane, S. B. Rane and B. B. Kale, *Sustain. Energy Fuels*, 2019, **3**, 3406-3414.
12. W. Fu, J. Wang, S. Zhou, R. Li and T. Peng, *ACS Appl. Nano Mater.*, 2018, **1**, 2923-2933.
13. Y. Mi, L. Wen, Z. Wang, D. Cao, R. Xu, Y. Fang, Y. Zhou and Y. Lei, *Nano Energy*, 2016, **30**, 109-117.
14. G. J. Lee, Y. C. Zheng and J. J. Wu, *Catal. Today*, 2018, **307**, 197-204.